

Title:

Gradual emergence of temporal structures depending on the distance between neighboring callers in natural habitat of male treefrogs

Authors

Ikkyu Aihara^{1,*}, Ryu Takeda², Masahiro Shirasaka³, Daichi Kominami⁴, Hiromitsu Awano⁵, and Masayuki Murata⁴

Affiliation:

1. Division of Information Engineering, Institute of Engineering, Information and Systems, University of Tsukuba, Ibaraki, 305-8573, Japan
2. SANKEN, Osaka University, Ibaraki, Osaka, 567-0047, Japan
3. Department of Computer Science, Graduate School of Systems and Information Engineering, University of Tsukuba, Ibaraki, 305-8573, Japan
4. Graduate School of Information Science and Technology, Osaka University, Osaka 565-0871, Japan
5. Graduate School of Informatics, Kyoto University, Kyoto, 606-8501, Japan

Corresponding author:

Ikkyu Aihara (aihara@cs.tsukuba.ac.jp)

Keywords:

Acoustic communication, Selective attention, Anti-phase synchronization, Call alternation

Abstract

Acoustic animals (e.g., insects and frogs) aggregate and produce sounds for mating. Well-organized chorus structures like call alternation and call synchrony indicate the importance of the precise control of call timing by individual males. However, the stable monitoring of multiple acoustic features in natural environments, especially the variation in call frequency, call timing and caller position, lacked in previous studies because of technical difficulties originating from the intense background noise, the existence of multiple sound sources and the wide area for monitoring. Here we have examined the spatio-temporal frequency structure in the choruses of wild treefrogs. First, we have performed field recordings by combining the sound-imaging system (25-66 units of sound-imaging devices) and microphone-array system (16-24ch of microphones) between 2021 and 2023. Second, we have analyzed the video and audio data and quantified the call frequency, call timing and caller position of each male, for 11 choruses with 66 males in total. Based on this large datasets, we have shown that synchronized behavior (call alternation) gradually emerges between neighboring callers depending on their distances even when the call frequency and chorus density moderately vary.

—

Introduction

Males of acoustic animals (e.g., insects and frogs) show well-organized behavior due to the interaction with other individuals for the purpose of mating. For instance, male frogs usually alternate their calls with neighbors (Aihara et al., 2011; Aihara et al., 2014; Brush and Narins, 1989; Gerhardt and Huber, 2002; Jones et al., 2014; Wells, 2007). Such a call alternation allows males to avoid acoustic interference and effectively advertise themselves towards conspecific females (Schwartz 1987; Legett et al. 2019). Male insects (e.g., katydids, crickets and cicadas) show both call synchrony and call alternation depending on species (Gerhardt and Huber, 2002; Sismondo 1990; Greenfield and Roizen, 1993; Greenfield et al., 2021; Cooley and Marshall 2001; Ishimaru and Aihara 2025). Call synchrony is known as the strategy to mask the acoustic signals of competitors and deteriorate their attractiveness (Cooley and Marshall 2001; Greenfield and Roizen 1993). In addition to the temporal structures, the frequency of acoustic signals plays an important role for mate attraction. Playback experiments have shown that females prefer the lower-frequency calls in some species (Ryan et al., 1992, Wollerman 1998, Giacoma et al., 1997; but see Gwynne and Bailey 1988); audio recordings with the measurement of body size have demonstrated that the call frequency is negatively correlated with the body size in general (Arak 1988; Morrison et al., 2001; Wollerman 1998; Giacoma et al., 1997; Gwynne and Bailey 1988). Thus, the temporal and frequency features of acoustic signals are the key factors in mating process.

In breeding seasons, males aggregate and show complicated spatial distributions in the wild. Given that males advertise their territories by producing sounds (Gerhardt and Huber, 2002; Wells 2007), the spatial distribution of acoustic animals can interact with their temporal chorus structure. Such an interaction due to the species-specific acoustic signals raises the important question "*what type of the spatio-temporal frequency structure is realized in natural environments*". Field observations showed that call alternation between neighbors is abundant in the choruses of male frogs (Brush and Narins 1989; Grafe 1996; Jones et al. 2014; Aihara et al. 2014), but the statistical analysis based on large datasets incorporating the variations in the chorus size and call frequency was not performed. Moreover, previous studies indicated that the well-organized structure between neighbors likely disappears when the chorus size becomes larger (Schwartz 1993; Schwartz et al. 2002). Hence, further studies on the chorus structures in natural environments are required. Recent advances in the technologies of audio recordings and signal processing allow us to estimate detailed features of acoustic signals and the positions of callers (Aihara et al. 2011; Au and Herzing, 2003; Fujioka et al., 2016; Grafe 1997; Jones et al. 2014; Rhinehart et al., 2020; Simmons et al. 2008; Suzuki et al., 2018). The application of such advanced technologies was proceeded especially

in wild bats and wild birds with large datasets (Fujioka et al., 2016; Suzuki et al., 2018) but the application to frogs and insects was relatively limited. Given the dense distribution of frogs and insects in breeding sites as well as their well-organized chorus patterns (e.g., call synchrony and call alternation), the stable monitoring of the spatio-temporal frequency structures can contribute to further understanding of the chorus dynamics in natural environments where acoustic communication is much difficult for animals due to the existence of multiple sound sources and the intense background noise.

Japanese treefrogs (*Hyla japonica*; *Dryophytes japonicus*; *Dryophytes leopardus*) distribute widely in Japan (Matsui and Maeda 2018). Male Japanese treefrogs are known to show well-organized temporal structures in their choruses. Laboratory experiments with a microphone array have demonstrated that two males tend to call alternately (Aihara 2009) while three males show tri-phase synchronization and clustered anti-phase synchronization (Aihara et al. 2011); field recordings with sound-imaging method have shown the occurrence of call alternation in the wild (Mizumoto et al., 2011; Aihara et al., 2014; Aihara et al., 2016). However, (1) the lack of larger datasets capturing the variance of spatial distributions and (2) the lack of frequency features especially in field sites precluded us from statistically testing the spatio-temporal frequency structures in their choruses. Given the well-organized temporal structure and the availability of advanced recording technologies that we have established for this species (Awano et al., 2021), the calling behavior of Japanese treefrogs is now worth further studying from the viewpoint of the spatio-temporal frequency structures of acoustic animals in the wild.

Materials and Methods

Field observations demonstrated that, at the beginning of breeding seasons, male Japanese treefrogs aggregate along the edges of rice paddies (Mizumoto et al. 2011; Aihara et al. 2014; Aihara et al., 2016) and produce advertisement calls in the form of unison bout (Aihara et al. 2019). To cover such a wide area with multiple sound sources that are synchronously activated, advanced methodologies for sound-source separation and localization are required. For that purpose, we combined two recording systems, (1) the sound-imaging system and (2) microphone-array system, that we had developed. The sound-imaging system consists of a device that is illuminated when detecting nearby sounds (Mizumoto et al., 2011; Awano et al., 2021). In the previous study, we deployed dozens of the devices along the edges of rice paddies and succeeded in estimating the position of callers and the time of their calls (Mizumoto et al., 2011; Aihara et al., 2014; Awano et al., 2021). While the sound-imaging system allows us to quantify the spatio-temporal structures in the choruses of male frogs, we could not estimate

the frequency of acoustic signals. In this study, we simultaneously set up a recording system consisting multiple microphone arrays that is aimed at the estimation of the acoustic frequency due to sound source separation. Each microphone array (System in Frontier Inc., TAMAGO) consists of eight microphones and is connected to a laptop computer for the precise control of audio recordings. There are vegetations around the rice paddy that can disturb the propagation of audio signals between the sound sources and microphones. To minimize the negative effect, we deployed the microphone arrays inside the rice paddy at almost the same height with the calling frogs.

Figure 1 schematically shows our recording system that was set up in natural environment. First, we deployed 25-66 units of the sound-imaging device along the edge of a rice paddy to cover the one-dimensional distribution of male treefrogs and recorded the illumination pattern of the devices by a video camera (SONY, HDR-PJ630) at the sampling rate of 60 fps (frames per second). The response frequency of the sound-imaging devices was tuned to the call frequency of the focal species in advance, according to the procedure of our previous study (Awano et al. 2021). Second, we deployed two or three units of the microphone array (16 or 24 microphones in total) inside the rice paddy by using miniature tripods (Ulanzi, MT-08) and recorded audio signals at the sampling rate of 48kHz by using laptop computers. This recording was repeated at 11 times between 2021 and 2023 (2nd, 10th, 11th, 14th, 16th and 18th, June 2021, 17th and 24th, June, 2022, and 14th, 16th and 30th, June 2023) at a paddy field in Ishioka city, Ibaraki, Japan ($36^{\circ} 18'01.5''N$ $140^{\circ} 10'32.7''E$).

We quantified the position of callers as well as the time and frequency of their calls from the video and audio data. First, we analyzed the video data according to the method of our previous study (Mizumoto et al., 2011; Aihara et al., 2014; Awano et al., 2021) and estimated the position of the devices [pixel] and the time [sec] when the LED of each device was activated by the calls of male treefrogs. The coordinate of each device [pixel] was converted to that in an actual space [cm] due to the method called *Homography* (Solem 2012; Aihara et al., 2017) by using four reference points that had been measured in advance by a laser distance meter (MAX Co. Ltd., LS-811). Consequently, we succeeded in detecting 66 males in total that constantly called during the field recording. Second, we applied the method of sound source separation to the audio data of the microphone arrays. We chose the section including the signals of multiple callers based on the illumination pattern of the sound-imaging devices, extracted the corresponding audio data of the microphone arrays, and carried out the sound-source separation due to the independent vector analysis (Kim et al. 2006) that is a well-established signal processing method for blind source separation (see Supplementary Information for details; see also Figure S2 of Supplementary Information for the demonstration of the sound source separation). Finally, we succeeded in estimating the

frequency of calls for all the identified callers (66 males in total) by using the separated audio signals.

To quantify the strength of synchronization for each pair of male frogs, we calculated the phase difference from the sequences of call time. The phase difference $\phi_{nm}(i)$ is defined as follows (Pikovsky et al 2001; Aihara et al 2011, 2014; Greenfield et al 2021):

$$\phi_{nm}(j) = 2\pi \frac{t_m(k) - t_n(j)}{t_n(j+1) - t_n(j)}, \quad (1)$$

where

$$t_n(j) \leq t_m(k) < t_n(j+1). \quad (2)$$

Here, $t_n(j)$ represents the time of the j th call produced by the n^{th} frog. Given the restriction of Equation (2), $\phi_{nm}(j)$ is limited to the range between 0 and 2π . This phase difference allows us to discriminate various temporal structures depending on its value. For example, call synchrony (i.e., in-phase synchronization) is described by $\phi_{nm}(j) = 0$ while call alternation (i.e., anti-phase synchronization) is described by $\phi_{nm}(j) = \pi$. Because Japanese treefrogs tend to call alternately (Aihara 2009; Aihara et al., 2011, 2014 and 2016), the distribution of the phase difference is expected to be localized around π . To quantify such a sharpness of the distribution of the phase difference, we define the following quantity according to the methodology of circular statistics (Fisher 1993; Kanji 1993):

$$\gamma_{nm} \exp(i\psi_{nm}) = \frac{1}{N} \sum_j \exp(i\phi_{nm}(j)). \quad (3)$$

Here, γ_{nm} and ψ_{nm} are the length and angle of the mean vector for the sequence of the phase difference $\phi_{nm}(j)$. For example, γ_{nm} takes the maximum value of 1 when the focal pair of calling males shows perfect synchronization and all the data of $\phi_{nm}(j)$ are the same; γ_{nm} is close to zero when the focal pair does not show synchronization and the data of $\phi_{nm}(j)$ are randomly distributed. To obtain a reliable mean vector from Equation (3), we restricted our analysis to the pair of males in which more than 300 samples of phase difference were obtained.

At last, we statistically examined the origin of temporal structures in frog choruses. Specifically, we used the following statistical model (the generalized linear model (Schall 1991; Faraway 2006)):

$$\gamma_{nm} \sim \text{Gamma}(\alpha, \beta), \quad (4)$$

and

$$\log\left(\frac{\alpha}{\beta}\right) = a_{\text{distance}}X_{\text{distance},nm} + a_{\text{freq}}X_{\text{freq},nm} + a_{\text{density}}X_{\text{density},nm} + a_0. \quad (5)$$

Here γ_{nm} is the length of the mean vector of the phase difference $\phi_{nm}(j)$ that gives the strength of synchronization. The definition of γ_{nm} (Equation (3)) means that this quantity takes a positive value, which is the reason why γ_{nm} is assumed to follow the Gamma distribution of Equation (4) with the log link function of Equation (5). The variables $X_{distance,nm}$, $X_{freq,nm}$ and $X_{density,nm}$ are the distance [m], the difference of call frequency [kHz], and the chorus density [Num. of callers/m] for the pair of the n^{th} and m^{th} frogs. Using the total length of one-dimensional distribution of the sound-imaging devices L_{dist} and the number of calling males along that line N_{caller} , the chorus density $X_{density,nm}$ was calculated as N_{caller}/L_{dist} . The ranges of $X_{distance,nm}$, $X_{freq,nm}$ and $X_{density,nm}$ were normalized between 0 and 1, allowing us to compare the magnitude relationship between the coefficients $a_{distance}$, a_{freq} and $a_{density}$. The unknown parameters of this model (i.e., $a_{distance}$, a_{freq} , $a_{density}$ and a_0) were estimated by Bayesian method from our empirical data of γ_{nm} , $X_{distance,nm}$, $X_{freq,nm}$ and $X_{density,nm}$ that had been obtained from 11 field recordings with 66 male treefrogs in total.

Results

The spatio-temporal frequency structures of frog choruses were quantified by our methodology combining the sound-imaging system and microphone-array system. Figure 2A and B shows the spatial distribution and illumination pattern of the sound-imaging devices, respectively. The devices activated by the calls are emphasized by pink plots (Figure 2A), corresponding to the positions of calling males. The illumination pattern of the devices captures the periodic calling behavior of each male (Figure 2B) that is consistent with the previous reports on this species (Matsui and Maeda 2018; Aihara 2009; Aihara et al., 2011, 2014 and 2016). Figure 2C shows a representative result of the sound source separation; the comparison of the separated audio signals with the illumination pattern of the sound imaging devices allows us to determine which device responded to each audio signal. At last, we estimated the frequency of the calls for each male by using the separated audio signals. The distribution of the dominant call frequency for all the frogs (66 males in total) shows an obvious peak around 3.4 kHz (see Figure S3 in Supplementary Information) that is consistent with the previous report on this species (Matsui and Maeda 2018).

Figure 3 shows representative spatio-temporal frequency structures in the choruses of male treefrogs. These are the examples of a relatively small chorus with three males that distributed along the edge of a rice paddy. In the first example of Figure 3A, neighboring pairs were located at the similar distance of about 2 m. The frequency of their calls moderately varied at 3.06, 3.33 and 3.39 kHz. The phase difference between neighbors was localized

around π , demonstrating the occurrence of call alternation (i.e., anti-phase synchronization). The second example of Figure 3B indicates the change in temporal chorus pattern depending on datasets. In particular, the spatial distribution was more asymmetric in this case: namely, the distance between the 1st and 2nd frogs was much shorter than that between the 2nd and 3rd frogs. Subsequently, the distribution of the phase difference between the 1st and 2nd frogs was much more peaky than that between the 2nd and 3rd frogs, indicating the effect of the spatial distribution on the temporal chorus structure.

To examine how the spatial frequency features affect the robustness of the temporal chorus pattern, we performed statistical analysis according to the procedure explained in *Materials and Methods*. Figure 4 summarizes the results of our analysis for two kinds of datasets: (1) the pairs of neighboring callers ($N = 81$ pairs) and (2) the pairs of distant callers ($N = 93$ pairs). As for the first dataset, the 95% confidence intervals (the 95% CIs) of $a_{distance}$ and $a_{density}$ are negative while the 95% confidence interval of a_{freq} includes zero (see the top panel of Figure 4A). The scatter plot with the estimated parameters shows obvious negative relationship between the inter-frog distance and the degree of synchronization (see the bottom panel of Figure 4A). We have also confirmed that the averaged phase difference is close to π when γ_{nm} is high, demonstrating the occurrence of call alternation between close neighbors (see Figure S4 in Supplementary Information). On the other hand, the absolute value of $a_{density}$ is much smaller than that of $a_{distance}$ and the upper limit of the 95% CI of $a_{density}$ is close to zero; this feature indicates that the effect of the chorus density is significant but much weaker and marginal. As for the second dataset, the 95% CIs of $a_{distance}$, $a_{density}$ and a_{freq} include zero, meaning that we could not detect any significant relationship. Thus, our analysis demonstrates that (1) synchronized behavior gradually emerged between close neighbors depending on their distances in natural environment and (2) the chorus density slightly weakened the strength of synchronization as for the pairs of neighboring callers.

Discussion

In this study, we examined the spatio-temporal frequency structures in the choruses of wild treefrogs (*H. japonica*; *D. japonicus*; *D. leopardus*). First, we performed field recordings by combining the sound-imaging system and the microphone-array system. Second, we analyzed the video and audio data and quantified the position of callers as well as the time and frequency of their calls. Our analysis using the statistical model showed that (1) the distance between neighboring callers dominantly affected the strength of synchronization even when the frequency and chorus density moderately varied and (2) the chorus density slightly

weakened the strength of synchronization as for the pairs of neighboring callers while its effect is much weaker than that of the inter-frog distance.

Here we discuss the biological contribution of this study. The spatio-temporal structures were examined in other species of frogs due to field recordings. Those studies indicated that call alternation is abundant in the choruses of male frogs (Brush and Narins 1989; Grafe 1996; Jones et al. 2014; Aihara et al. 2014) but the statistical analysis based on large datasets incorporating the variations in the chorus size and call frequency was not performed. In addition, previous studies indicated that the well-organized structure between neighbors disappears when the chorus size becomes larger (Schwartz 1993; Schwartz et al. 2002). This study has shown that synchronized behavior (call alternation) emerges between close neighbors depending on their distances even when the frequency and chorus density vary, indicating the high ability in the acoustic communication of the wild treefrogs in natural environment. It should be noted that we have also detected a significant negative effect of the chorus density on the strength of synchronization; this result seems consistent with the previous studies on the chorus size (Schwartz 1993; Schwartz et al. 2002) although the effect of the chorus density has been estimated to be much weak in the case of Japanese treefrogs.

Next, we discuss the technical contribution of our methodology from the viewpoint of applications. In this study, we have succeeded in quantifying the spatio-temporal frequency structures in the choruses of wild treefrogs by combining two recording systems, i.e., the sound-imaging system and microphone-array system. Such a sound-source separation and localization in natural environment are applicable to various systems. One of the plausible applications is the audio recording of other animals. Various species of insects and frogs aggregate and produce sounds for mating (Gerhardt and Huber, 2002; Wells, 2007) like Japanese treefrogs, which requires the advanced technology for sound-source localization and separation. Humans also aggregate and talk with each other for the purpose of meetings, daily conversations and parties; the acoustic features of each person (e.g., the speech amount) have been evaluated by using a microphone array (Nagira and Mizumoto 2023; Hashimoto et al. 2025) for the purpose of the quantification of human communications. Another scenario of the applications is disaster robotics (Tadokoro 2019). In disaster sites, the positions of injured people are unknown and need to be identified on the basis of their voices. Array signal processing technologies have been developed or designed for multiple types of robots, such as drones (Ohata et al 2014; Yamada et al 2021) and a hose-shaped rescue robot (Bando et al 2009). The point is that our methodology has accomplished sound-source separation and localization in natural frog choruses which form quite intense noise originating from acoustically similar sources across the wide area. Consequently, this study can contribute to the development of methodologies for sound-source separation and localization that can work

in acoustically complicated natural environments.

Acknowledgement

We are grateful to Mr. Akira Mutazono to allow us to perform field recordings at his rice paddy. We appreciate Mr. Takahiro Ishimaru, Mr. Toma Ishiduki, Mr. Kosei Murakoso and Mr. Makoto Nashiki for their assistance on field works. All the experiments were performed in accordance with the guideline of the Animal Experimental Committee of University of Tsukuba. This study was partially supported by Grant-in-Aid for Scientific Research (B) (No.20H04144), "Innovation inspired by Nature" Research Support Program, SEKISUI CHEMICAL CO. LTD, and SECOM Science and Technology Foundation.

Figure

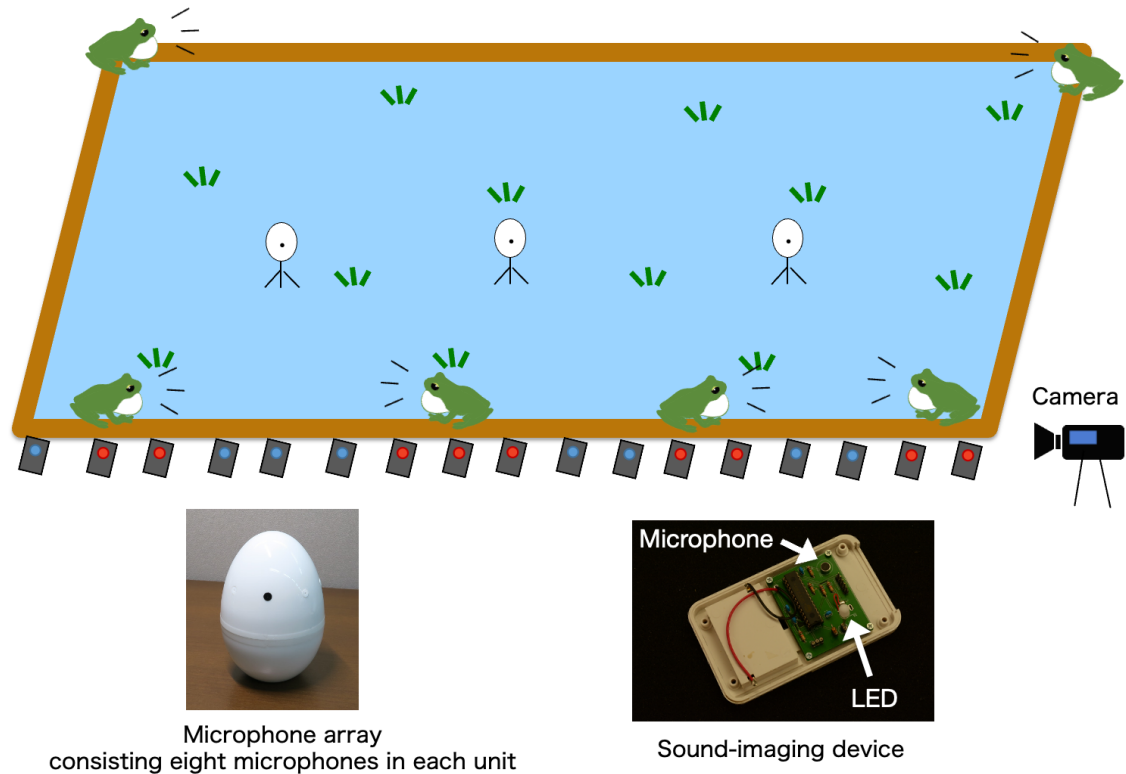


Figure 1: Schematic diagram of our recording system consisting of the sound-imaging devices and microphone arrays. Given the one-dimensional distribution of Japanese tree frogs (*Hyla japonica*; *Dryophytes japonicus*; *Dryophytes leopardus*), we deployed the sound-imaging devices along the edge of a rice paddy. To record the audio signals of the treefrogs at a high signal-to-noise ratio, we set multiple microphone arrays inside the rice paddy at the similar height with the calling frogs. This recording was repeated at 11 times between 2021 and 2023, enabling us to detect 66 callers in total.

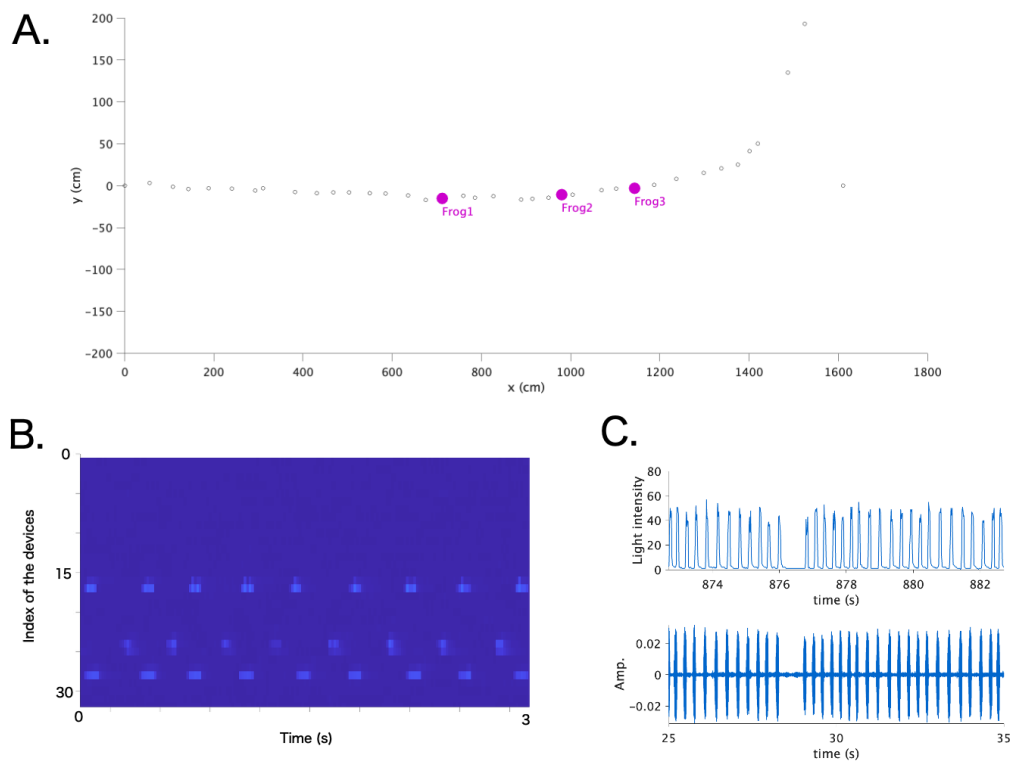


Figure 2: Quantification of chorus patterns from the field recordings. (A) The positions of the sound-imaging devices estimated from video data. The devices illuminated by the calls of male treefrogs are emphasized by pink plots while other devices are indicated by open dots. (B) Illumination patterns of the sound-imaging devices. The time series data of the illuminance allow us to estimate the time when each call was produced. (C) Sound-source separation from the audio data. The separated audio signals (bottom panel) are consistent with the illumination pattern of the focal device (top panel), demonstrating the validity of the sound-source separation. The frequency of calls was estimated from the separated audio signals for each male frog.

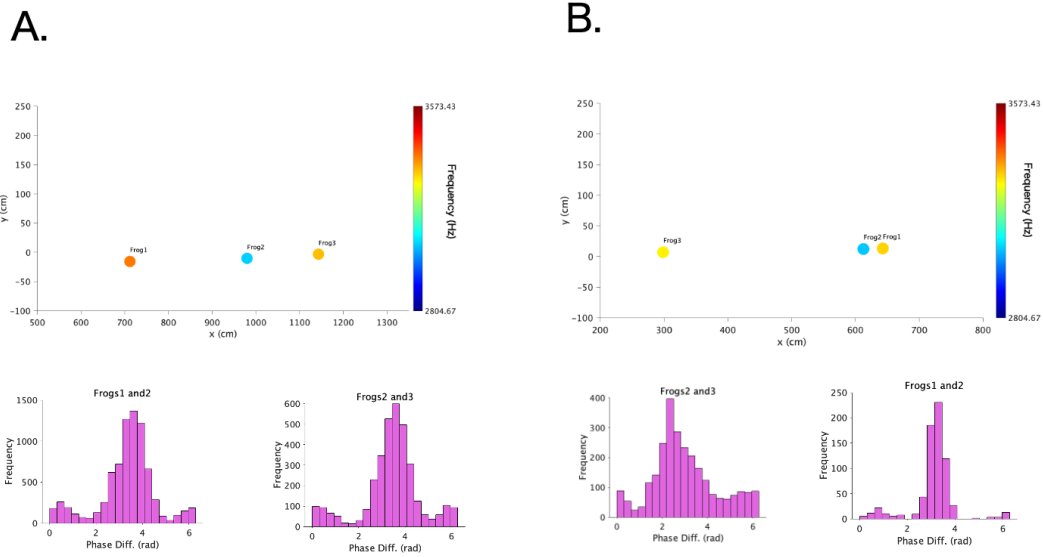
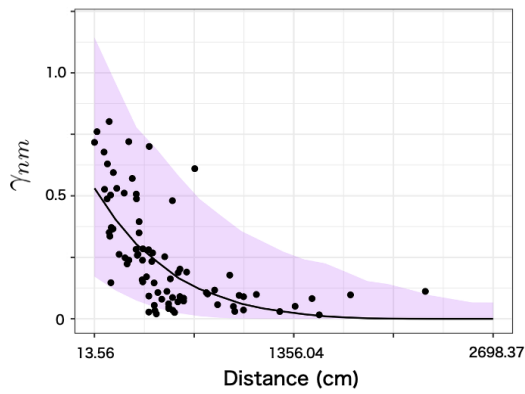


Figure 3: Representative spatio-temporal frequency structures in frog choruses. These are two examples of a relatively small chorus with three males. In both figures, colored plots represent the positions of callers with the frequency of their calls. The histograms show the distributions of the phase differences between neighbors. In the example of Figure 4A, the distance between the 1st and 2nd frogs is close to that between the 2nd and 3rd frogs; the distributions of the phase differences are similar. In contrast, the spatial structure is more asymmetric in the example of Figure 4B; the distribution of the phase difference between close neighbors (the 1st and 2nd frogs) is more peaky than that between distant neighbors (the 2nd and 3rd frogs). This comparison indicates the effect of the spatial structure on the strength of synchronization.

A. The pairs of neighboring callers



Parameter	Posterior Mean	95% CI	Rhat
$a_{distance}$	-4.86	-6.40 ~ -3.40	1.00
a_{freq}	+0.09	-0.51 ~ +0.69	1.00
$a_{density}$	-0.43	-0.84 ~ -0.04	1.00
a_0	-0.58	-0.91 ~ -0.26	1.00



B. The pairs of distant callers



Parameter	Posterior Mean	95% CI	Rhat
$a_{distance}$	-0.47	-1.19 ~ +0.21	1.00
a_{freq}	-0.21	-0.72 ~ +0.31	1.00
$a_{density}$	-0.08	-0.48 ~ +0.31	1.00
a_0	-2.30	-2.67 ~ -1.96	1.00

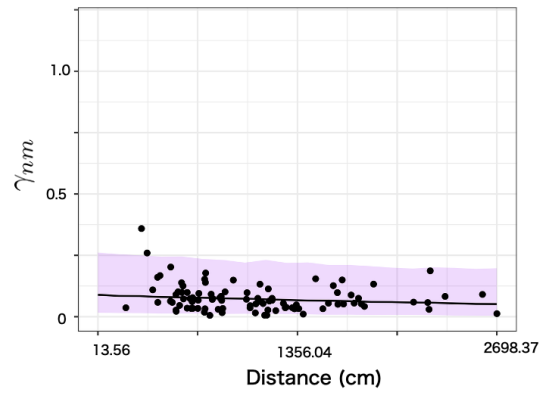


Figure 4: Statistical analysis on the spatio-temporal frequency structures by using two kinds of datasets: (A) the pairs of neighboring callers ($N = 81$) and (B) the pairs of distant callers ($N = 93$). Top panels represent the tables of the parameter estimation and bottom panels represent the scatter plots with the estimated model parameters. As for the pairs of neighboring callers, the inter-frog distance and chorus density significantly affect the strength of synchronization (γ_{nm}). In the contrast, there was no significant relationship as for the pairs of distant callers. In the bottom panels, the horizontal axis was rescaled for the actual length (cm) while the parameter estimation was carried out on the basis of normalized variables (see Materials and Methods for details).

Reference

- Aihara, I. (2009). Modeling synchronized calling behavior of Japanese tree frogs. *Physical Review E—Statistical, Nonlinear, and Soft Matter Physics*, 80(1), 011918.
- Aihara, I., Takeda, R., Mizumoto, T., Otsuka, T., Takahashi, T., Okuno, H. G. and Aihara, K. (2011). Complex and transitive synchronization in a frustrated system of calling frogs. *Phys. Rev. E* **83**, 031913.
- **Aihara, I., Mizumoto, T., Otsuka, T., Awano, H., Nagira, K., Okuno, H. G. and Aihara, K.** (2014). Spatio-temporal dynamics in collective frog choruses examined by mathematical modeling and field observations. *Sci. Rep.* **4**, 1–8.
- Aihara, I., Mizumoto, T., Awano, H., & Okuno, H. G. (2016). Call Alternation Between Specific Pairs of Male Frogs Revealed by a Sound-Imaging Method in Their Natural Habitat. Proceedings of *INTERSPEECH* (pp. 2597-2601).
- Aihara, I., Kominami, D., Hirano, Y., & Murata, M. (2019). Mathematical modelling and application of frog choruses as an autonomous distributed communication system. *Royal Society open science*, 6(1), 181117.
- Arak, A. (1988). Female mate selection in the natterjack toad: active choice or passive attraction?. *Behavioral Ecology and Sociobiology*, 22(5), 317-327.
- **Au, W. W. L. and Herzing, D.L.** (2003). Echolocation signals of wild Atlantic spotted dolphin (*Stenella frontalis*). *J. Acoust. Soc. Am.* **113**, 598–604.
- Awano, H., Shirasaka, M., Mizumoto, T., Okuno, H. G., & Aihara, I. (2021). Visualization of a chorus structure in multiple frog species by a sound discrimination device. *Journal of Comparative Physiology A*, 207(1), 87-98.
- Bando Y., Ambe Y., Itoyama K., and Okuno H.G. (2019), Extreme Audition for Active Scope Camera, *Journal of the Robotics Society of Japan*, Volume 37, Issue 9, Pages 808-813, in Japanese.
- **Brush, J.S. and Narins, P. M.** (1989). Chorus dynamics of a neotropical amphibian assemblage: comparison of computer simulation and natural behaviour. *Anim. Behav.* **37**, 3344.
- **Cooley, J. R., & Marshall, D. C.** (2001). Sexual signaling in periodical cicadas, *Magicicada* spp. (Hemiptera: Cicadidae). *Behaviour*, 827-855.
- Faraway JF. 2006 Extending the linear model with R. Boca Raton, FL: CRC Press.
- **Fisher, N. I.** (1993). *Statistical analysis of circular data*. Cambridge, UK: Cambridge University Press.
- **Fujioka, E., Aihara, I., Sumiya, M., Aihara, K. and Hiryu, S.** (2016). Echolocating bats use future target information for optimal foraging. *Proc. Natl. Acad. Sci. USA* **113**, 4848–

4852.

- Gerhardt, H. C. & Huber, F. Acoustic Communication in Insects and Anurans. (University of Chicago Press, 2002).
- **Grafe, T. U.** (1996). The function of call alternation in the African reed frog (*Hyperolius marmoratus*): precise call timing prevents auditory masking. Behavioral Ecology and Sociobiology, 38, 149-158.
- **Grafe, T.U.** (1997) Costs and benefits of mate choice in the lek-breeding reed frog, *Hyperolius marmoratus*. Anim. Behav. **53**, 1103–1117.
- **Greenfield, M. D. and Roizen, I.** (1993). Katydid synchronous chorusing is an evolutionarily stable outcome of female choice. *Nature* **364**, 618–620.
- **Greenfield, M. D., Aihara, I., Amichay, G., Anichini, M. and Nityananda, V.** (2021). Rhythm interaction in animal groups: selective attention in communication networks. *Philos. Trans. R. Soc. B*, **376**(1835), 20200338.
- Hashimoto E., Nagira K., Mizumoto T., and Shiramatsu S. (2025). Human Capital Visualization using Speech Amount during Meetings. In Proceedings of the 26th Annual Meeting of the Special Interest Group on Discourse and Dialogue, pages 441–448, Avignon, France. Association for Computational Linguistics.
- Kanji G. K., 100 Statistical tests (SAGE Publications Ltd, 1993).
- **Höbel, G., & Gerhardt, H. C.** (2007). Sources of selection on signal timing in a tree frog. *Ethology*, 113(10), 973-982.
- Ishimaru, T., & Aihara, I. (2025). Temporal structure of two call types produced by competing male cicadas. *Journal of Experimental Biology*, 228(8), jeb249399.
- **Jones, D. L., Jones, R. L. and Ratnam, R.** (2014). Calling dynamics and call synchronization in a local group of unison bout callers. *J. Comp. Physiol. A* **2001**, 93107.
- Kim T., Eltoft T., and Lee T. (2006). Independent vector analysis: an extension of ICA to multivariate components. In Proceedings of the 6th international conference on Independent Component Analysis and Blind Signal Separation (ICA'06).
- Legett, H. D., Page, R. A., & Bernal, X. E. (2019). Synchronized mating signals in a communication network: the challenge of avoiding predators while attracting mates. *Proceedings of the Royal Society B*, 286(1912), 20191067.
- Matsui and Maeda. Encyclopedia of Japanese frogs. (Bun-ichi Sogo Shuppan Co., Ltd., 2018).
- **Mizumoto, T., Aihara, I., Otsuka, T., Takeda, R., Aihara, K., & Okuno, H. G.** (2011). Sound imaging of nocturnal animal calls in their natural habitat. *Journal of Comparative Physiology A*, 197(9), 915-921.
- Nagira K. and Mizumoto T. (2023). Quantitative visualization of online or face-to-face

discussions for reflection. In The 37th Annual Conference of the Japanese Society for Artificial Intelligence, 4R3-OS-22b-03. (in Japanese).

- Ohata T., Nakamura K., Mizumoto T., Taiki T., and Nakadai K., Improvement in outdoor sound source detection using a quadrotor-embedded microphone array, *2014 IEEE/RSJ International Conference on Intelligent Robots and Systems*, Chicago, IL, USA, 2014, pp. 1902-1907, doi: 10.1109/IROS.2014.6942813.
- Pikovsky, A., Rosenblum, M. & Kurths, J. Synchronization: A Universal Concept in Nonlinear Sciences (Cambridge University Press, Cambridge, 2001).
- Rhinehart, T. A., Chronister, L. M. and Devlin, T. (2020). Acoustic localization of terrestrial wildlife: current practices and future opportunities. *Ecol. Evol.* **10**,1–25.
- Schall R. 1991 Estimation in generalized linear-models with random effects. *Biometrika* 78,719–727.
- Schwartz, J. J. (1987). The function of call alternation in anuran amphibians: a test of three hypotheses. *Evolution*, 41(3), 461-471.
- Schwartz, J. J. (1993). Male calling behavior, female discrimination and acoustic interference in the Neotropical treefrog *Hyla microcephala* under realistic acoustic conditions. *Behavioral Ecology and Sociobiology*, 32(6), 401-414.
- **Schwartz, J. J., Buchanan, B. W., & Gerhardt, H.** (2002). Acoustic interactions among male gray treefrogs, *Hyla versicolor*, in a chorus setting. *Behavioral Ecology and Sociobiology*, 53, 9-19.
- **Simmons A. M., Simmons J. A., Bates M. E.** (2008) Analyzing acoustic interactions in natural bullfrog (*Rana catesbeiana*) choruses. *J. Comp. Psychol.* 122, 274–282.
- **Suzuki, R., Matsubayashi, S., Saito, F., Murate, T., Masuda, T., Yamamoto, K., Kojima, R., Nakadai, K. and Okuno, H. G.** (2018). A spatiotemporal analysis of acoustic interactions between great reed warblers (*Acrocephalus arundinaceus*) using microphone arrays and robot audition software HARK. *Ecol. Evol.* **8**, 812–825.
- **Sismondo, E.** (1990). Synchronous, alternating, and phase-locked stridulation by a tropical katydid. *Science*, 249(4964), 55-58.
- Tadokoro S. (2019). Overview of the ImPACT Tough Robotics Challenge and Strategy for Disruptive Innovation in Safety and Security. *Disaster Robotics: Results from the ImPACT Tough Robotics Challenge*. pp. 3-22.
- Wells, K. D. *The Ecology and Behavior of Amphibians*. (The University of Chicago Press, Chicago, 2007).
- Yamada T., Itoyama K., Nishida K. and Nakadai K. (2021). Assessment of Sound Source Tracking Using Multiple Drones Equipped with Multiple Microphone Arrays. *Int. J. Environ. Res. Public Health* 2021, 18, 9039. <https://doi.org/10.3390/ijerph18179039>

Supplementary Information

—

Sound-source separation

Blind source separation (BSS) is a signal processing method that separates an observed mixture of source signals into isolated ones. We need only the recorded audio data in multi-channel: the positions of microphones and sound sources are not required in advance while traditional beamformers do. The assumption of the method is a statistical property of source signals, such as independence among sound sources, that will satisfy almost all sound sources in the real world. The advantage on the few assumptions makes BSSs a useful tool of sound signals for the non-experts of signal processing.

We simply explain the mixing process between the observed signals at microphones and sound sources. We denote the sound signals captured at each microphone i as $\mathbf{x}_t = [x_{t1}, \dots, x_{ti}, \dots, x_{tM}]$ where t represents a discrete time. $\mathbf{s}_t = [s_{t1}, \dots, s_{tj}, \dots, s_{tN}]$ represent a sound source vector whose element s_{tj} is a j -th source signal at time t . The sound wave propagates from sound sources to microphones with power decay and superposition via multiple paths. Such process can be modeled as

$$\mathbf{x}_t = \sum_d \mathbf{H}_d \mathbf{s}_t \quad (\text{S1})$$

where \mathbf{H}_d represents a so-called transfer function matrix of acoustic signal. Because we have observed signals from time t_a to t_b (for several seconds), we can utilize statistical information of sound signals.

Our purpose is to estimate the source vector \mathbf{s}_t from the observed vector \mathbf{x}_t . The independent vector analysis (IVA) is a kind of BSSs in the short-time Fourier transformation (STFT) domain (Kim et al., 2006; see Figure S1 for the schematic diagram of IVA). In the STFT domain, the convolution can be approximated by the multiplication of transfer function \mathbf{H}_w and source spectrum \mathbf{s}_{wf} , where w and f mean frequency-bin and frame indices of spectrum, respectively.

$$\mathbf{x}_{wf} = \mathbf{H}_w \mathbf{s}_{wf}, \quad (\text{S2})$$

The estimated source vector $\hat{\mathbf{s}}_{wf}$ can be obtained by multiplying separation matrix \mathbf{W}_w estimated by IVA to the observed vector \mathbf{x}_{wf} as follows:

$$\hat{\mathbf{s}}_{wf} = \mathbf{W}_w \mathbf{x}_{wf}, \quad (\text{S3})$$

The time-domain signals corresponding to the separated vectors are resynthesized through inverse STFT.

The estimation of separation filter \mathbf{W}_w is achieved by formulating as an optimization problem. Major formulations are the maximization of the likelihood or minimization of KL-divergence. Common factor is the design of the probabilistic density function (PDF) of sound sources. IVA uses a PDF of source vector along the frequency-axis, which overcomes a so-called permutation problem in the STFT processing of independent component analysis (ICA). Please see the detailed estimation algorithm in (Kim et al., 2006).

Figure legend

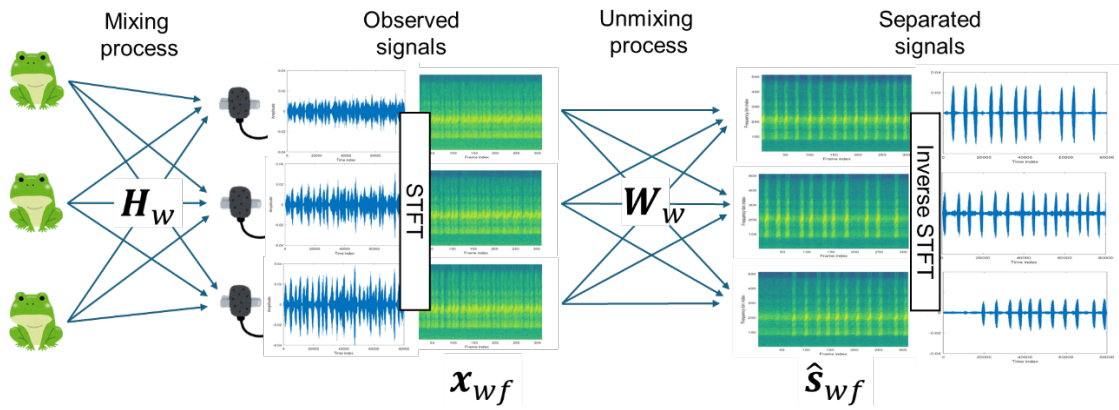
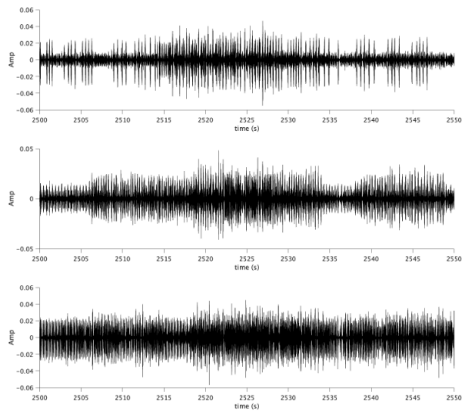


Figure S1: Schematic diagram of the independent vector analysis (IVA) on the assumption of multiple sound sources and microphones.

A.



B.

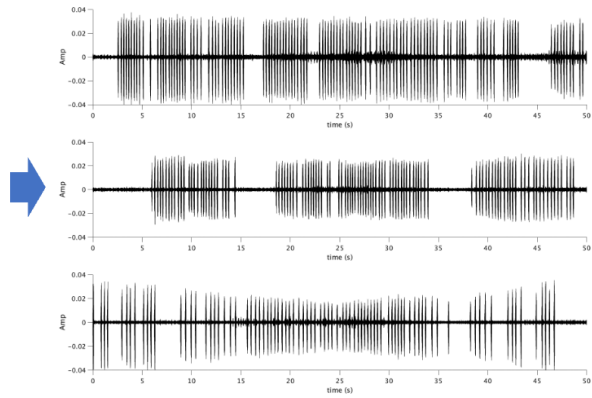


Figure S2: Representative result of the sound source separation. (A) Original audio data obtained from microphone arrays. (B) Separated audio signals obtained from the blind source separation (IVA). Separated audio signals show strong periodicity around 0.3 sec that is consistent with the previously reported behavior in this species (Matsui and Maeda 2018; Aihara 2009; Aihara et al., 2011, 2014 and 2016).

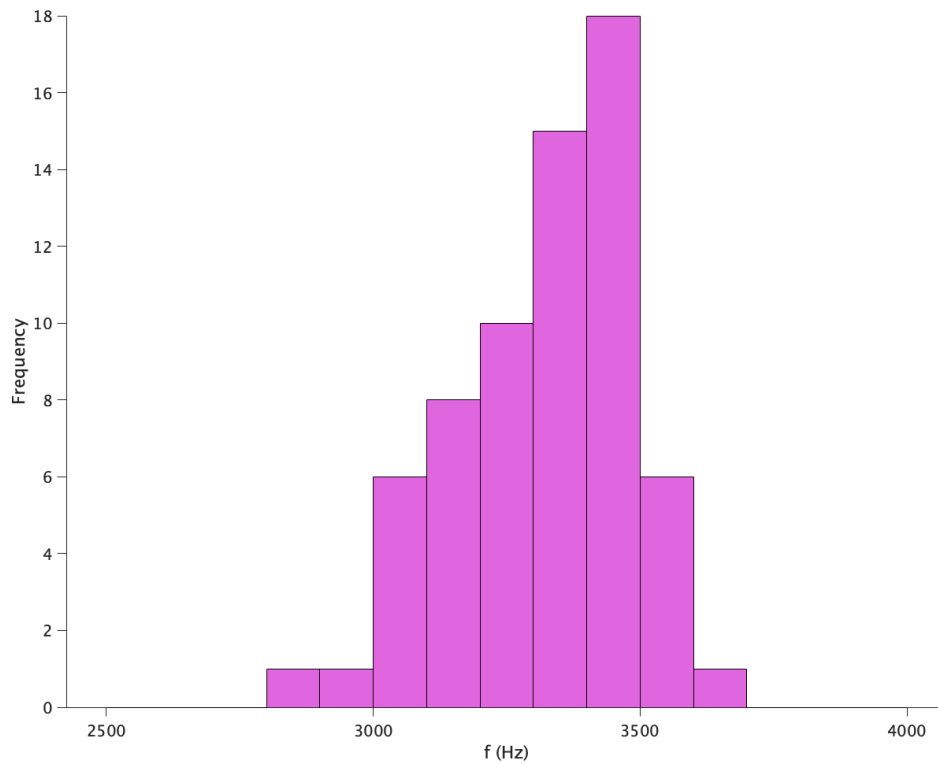


Figure S3: The histogram of the dominant call frequency in male treefrogs (N=66 males in total). There is an obvious peak around 3.4 kHz that is consistent with the dominant call frequency reported in this species (Matsui and Maeda 2018).

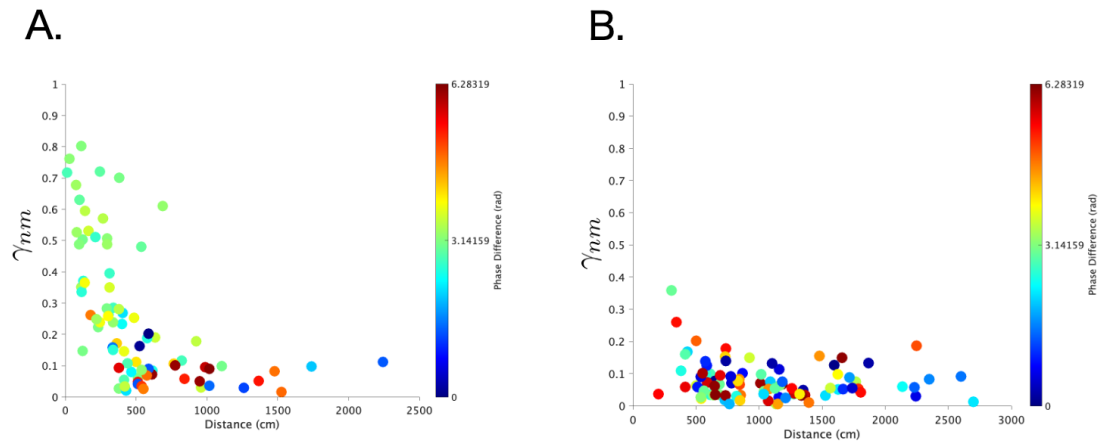


Figure S4. The scatterplot of the inter-frog distance and the strength of synchronization as for two kinds of datasets: (A) the pairs of neighboring callers and (B) the pairs of distant callers. A color gradient represents the value of the averaged phase difference. It is confirmed that the average phase difference is close to π when the strength of synchronization γ_{nm} is high.

Reference

- Aihara, I. (2009). Modeling synchronized calling behavior of Japanese tree frogs. *Physical Review E—Statistical, Nonlinear, and Soft Matter Physics*, 80(1), 011918.
- Aihara, I., Takeda, R., Mizumoto, T., Otsuka, T., Takahashi, T., Okuno, H. G. and Aihara, K. (2011). Complex and transitive synchronization in a frustrated system of calling frogs. *Phys. Rev. E* **83**, 031913.
- **Aihara, I., Mizumoto, T., Otsuka, T., Awano, H., Nagira, K., Okuno, H. G. and Aihara, K.** (2014). Spatio-temporal dynamics in collective frog choruses examined by mathematical modeling and field observations. *Sci. Rep.* **4**, 1–8.
- Aihara, I., Mizumoto, T., Awano, H., & Okuno, H. G. (2016). Call Alternation Between Specific Pairs of Male Frogs Revealed by a Sound-Imaging Method in Their Natural Habitat. Proceedings of *INTERSPEECH* (pp. 2597-2601).
- Kim T., Eltoft T., and Lee T-W. 2006. Independent vector analysis: an extension of ICA to multivariate components. In Proceedings of the 6th international conference on Independent Component Analysis and Blind Signal Separation (ICA'06).
- Matsui and Maeda. Encyclopedia of Japanese frogs. (Bun-ichi Sogo Shuppan Co., Ltd., 2018).